



# HHS Public Access

## Author manuscript

*Int J Min Sci Technol.* Author manuscript; available in PMC 2020 July 31.

Published in final edited form as:

*Int J Min Sci Technol.* 2020 January ; 30(1): 111–118. doi:10.1016/j.ijmst.2019.12.020.

## Analysis of ARMPS2010 database with LaModel and an updated abutment angle equation

**Deniz Tuncay<sup>a,\*</sup>, Ihsan Berk Tulu<sup>a</sup>, Ted Klemetti<sup>b</sup>**

<sup>a</sup>Department of Mining Engineering, West Virginia University, Morgantown, WV 26505, USA

<sup>b</sup>National Institute for Occupational Safety and Health, Pittsburgh Mining Research Division, Pittsburgh, PA 15236, USA

### Abstract

The Analysis of Retreat Mining Pillar Stability (ARMPS) program was developed by the National Institute for Occupational Safety and Health (NIOSH) to help the United States coal mining industry to design safe retreat room-and-pillar panels. ARMPS calculates the magnitude of the in-situ and mining-induced loads by using geometrical computations and empirical rules. In particular, the program uses the “abutment angle” concept in calculating the magnitude of the abutment load on pillars adjacent to a gob. In this paper, stress measurements from United States and Australian mines with different overburden geologies with varying hard rock percentages were back analyzed. The results of the analyses indicated that for depths less than 200 m, the ARMPS empirical derivation of a 21° abutment angle was supported by the case histories; however, at depths greater than 200 m, the abutment angle was found to be significantly less than 21°. In this paper, a new equation employing the panel width to overburden depth ratio is constructed for the calculation of accurate abutment angles for deeper mining cases. The new abutment angle equation was tested using both ARMPS2010 and LaModel for the entire case history database of ARMPS2010. The new abutment angle equation to estimate the magnitude of the mining-induced loads used together with the LaModel program was found to give good classification accuracies compared to ARMPS2010 for deep cover cases.

### Keywords

Abutment angle; ARMPS2010; LaModel; ARMPS-LAM; Coal mining; Pillar stability

### 1. Introduction

In the early 1990 s, the Analysis of Longwall Pillar Stability (ALPS) was introduced by Mark as a chain pillar design software and was generally accepted and used by the United States coal mining industry [1]. Following the success of ALPS, the National Institute for Occupational Safety and Health (NIOSH) developed the Analysis of Retreat Mining Pillar Stability (ARMPS) program for designing retreat mining pillars using a similar approach as

This is an open access article under the CC BY-NC-ND license (<http://creativecommons.org/licenses/by-nc-nd/4.0/>).

\*Corresponding author. dt0036@mix.wvu.edu (D. Tuncay).

ALPS [2]. The Australian mining industry also recognized the success of ALPS, and Colwell et al. calibrated the program to Australian conditions [3]. The ALPS and ARMPS programs draw their strengths from the large databases that are used to calibrate them [4]. However, following the Crandall Canyon Mine collapse in 2007, NIOSH had to reconsider the pillar design criteria used in deep-cover retreat mining [5]. The ARMPS overburden load prediction algorithm was improved to more accurately predict the loading of narrow panels with high overburden depths by implementing the pressure arch concept, and this new version is called ARMPS2010.

The LaModel program is generally used in the United States coal mining industry to model the stresses and displacements for complex mine geometries, multiple-seam coal mines, and topographic relief which cannot be analyzed accurately by ARMPS2010 or ALPS. LaModel is a displacement-discontinuity (DD) variation of the boundary element method, and because of this formulation, the program can analyze large areas of single- or multiple-seam coal mines [6]. LaModel is unique among boundary element codes because the overburden material includes lithologic laminations which give the model a very realistic flexibility for stratified sedimentary geologies and multiple-seam mines. Using LaModel, the total vertical stresses and displacements in the coal seam are calculated. Following the Crandall Canyon Mine collapse in 2007, Heasley et al. emphasized the importance of calibrating a numerical model [7]. It was stated that the accuracy of the input parameters greatly affects the success and accuracy of a LaModel analysis. Default properties provided by LaModel for the input parameters are applicable for average mining conditions and were developed to give reasonable results. However, site-specific conditions should be considered, and the default parameters should be modified if necessary. The first approximation of the overburden load is calibrated to mirror those used in ALPS and ARMPS2010, which is the best available information; however, the flexure of the laminated overburden and the relative stiffness/strength of the seam elements ultimately determine the final distribution of the overburden load [7]. Also, a previous study by Tulu and Heasley showed that the laminated overburden model calculated larger abutment extents compared to the original ALPS equation [8].

Using the LaModel calibration method with a relatively small deep-cover database, the LaModel program was shown to classify the case histories slightly better than ARMPS2010 [9]. The analysis for the laminated model was conducted by a program called ARMPS-LAM, which has the laminated overburden model integrated with ARMPS2010. ARMPS-LAM takes the basic geometric input like that of ARMPS2010 and develops, grids, and runs a LaModel analysis of the mining geometry. It outputs the section stability factor (SF) without the requirement for further user input. Comparison between ARMPS2010 and ARMPS-LAM has been investigated by Zhang et al., and it was concluded that the ARMPS-LAM was more successful for shallow cover cases with less than 304.80 m overburden [10]. Both ARMPS2010 and ARMPS-LAM are used in this study to test the performance of the newly suggested abutment angle equation.

## 2. Abutment angle concept

The abutment angle concept is used to calculate the magnitude of abutment loading adjacent to a gob area in the ALPS and ARMPS programs. LaModel also utilizes similar calculations

as part of its calibration process because the abutment angle equations are determined as the best available methods for estimating abutment loads. The concept considers an angle between the vertical plane and the panel roof in order to calculate the transferred load to the abutments when the panel is mined (Fig. 1).

In 1990, Mark analyzed the abutment stress measurements collected from five different mines [1]. All measurements were conducted using vibrating wire stressmeters (VWS). The United States Bureau of Mines (USBM) conducted three of the studies, all of which were conducted in the Pittsburgh seam. The fourth study was conducted by the Pennsylvania State University in the Lower Kittanning seam, and United States Steel conducted the fifth study at a mine operating in the Harlan seam. Mark back-calculated the measured side abutment load by multiplying the load-bearing area of the pillars by average pillar stresses determined from the array of stress cells inside each pillar [11,12]. A summary of the panel widths and depths from the case histories that were used by Mark to back-calculate the abutment angles from the case histories is shown in Table 1 [1]. Originally, a total of 16 stressmeter arrays were installed in five different mines, but side abutment measurements were available only from six arrays due to some of the meters being destroyed once the longwall had passed an array. That is why Table 1 only has data from four different mines. Mark concluded that an average abutment angle of  $21^\circ$  would yield a conservative estimate of the side abutment load, but there was a wide range ( $10.7^\circ$  to  $25.2^\circ$ ) in the measured values as seen in Table 1 [12].

Currently, active mines have significantly different panel dimensions as compared to the mines where the data were collected for the derivation of the abutment extent formula and the  $21^\circ$  average abutment angle. More recent in-situ stress measurements of abutment loading conducted in Australia and in the United States showed that there can be significant deviations in the measured abutment magnitude and extent, as compared to the predicted values from the present empirical formulas used in ALPS, ARMPS, and LaModel [3,13]. In addition, the presence of massive stiff units, their thickness, and their locations within the strata play an important role in load transfer. Massive stiff units can transfer loads to higher distances by resisting caving, hence reducing the expected loading of the gob [14,15]. In a study conducted by Van Dyke et al., it was found for their case that, within the first 15 m of roof, the presence of a more than 12-m-thick sandstone would be too strong to cave [16]. Another factor mentioned in the study was the caving height, which would have a direct effect on the cushioning of the massive sandstone above. Both factors are governed by the geologies of the roof layers, which would affect the load distribution around the panels. Recent studies show that site-specific overburden geology, seam thickness, and extraction of the panel width have a significant effect on the extent and magnitude of the abutment load, but these parameters are not included in the empirical calculations.

### 3. Re-analysis of abutment angle

#### 3.1. Stress measurements database

The mine cases used to derive the default  $21^\circ$  abutment angle have significantly narrower panel dimensions and relatively shallower overburden depths than most modern longwall panels. The original empirical abutment formulas were derived from the stress

measurements collected from these mines and have not been updated to include the changes in mine dimensions. In this paper, more recent in-situ stress measurements are used to re-examine abutment loads with consideration of geology.

Table 1 shows that the recommended abutment angle was calculated from measurements from panels shallower than 230 m, with most panels 183-m-wide or less.

To re-examine the abutment angle, a database was developed with the addition of more recent stress measurements. Six stress measurement case histories from Colwell et al. and another six case histories from Hill were added to the database [3,17]. In addition to these cases and the ones studied by Mark, another ten supplementary cases from Colwell et al. were added where only the total side abutment loads were known [1,3]. Twenty of the 28 additional case histories are from Australian longwall mines, and the remaining 8 cases are from United States longwall mines. Table 2 shows the statistical summary for the 28 case histories used in this study.

### 3.2. Geological settings and mining geometries

Out of the 28 cases, 12 cases that have the full side abutment measurements have been further analyzed. Of those 12 cases, 10 cases are from different mines. One is operated in the United States and 9 of them are from Australian mines. Geologic core logs were available for 8 of the mines, and more information on the geology was gathered from consulting reports. Fig. 2 shows the generalized stratigraphic columns of the case study sites, where enough information about the geology was present. Layers with more than one rock type represent interbedded or intermixed components, but the percentages may vary. Also, thick layers do not necessarily represent massive rock formations. Adjacent thin layers of the same rock types are combined for easier representation.

The available core logs and descriptions of the geologies from the reports were used to determine the hard rock (HR) percentage of the overlying strata for each case. Hard rock percentage is calculated considering the thickness of hard rock (sandstone and limestone) that is higher than 1.5 m from the core log [18]. It is the ratio of the length of hard rock core that is longer than 1.5 m to the total length of the core log above the coal seam. This methodology for defining the hard rock percentage was originally developed by Agioutantis and Karmis and used successfully in predicting subsidence magnitude and profile for the United States coal mines [18]. The following is a list of the case studies with the mine geometries and available geologic information, and Table 3 shows the summary of the cases.

AU1 mine: The AU1 mine's coal seam varies in thickness from 1.8 to 2.7 m. The overlying strata mostly consist of sandstone and laminate units. Enough information was not available to construct a representative stratigraphic column; however, the geologic formations that were present in the immediate roof were known. The depth of cover around the instrumentation site is approximately 265 m. The chain pillars are developed on  $45 \times 100$  m centers with a 5.0 m entry width and the panel is 205 m wide. The immediate floor is strong with minimum slaking potential. There were no stratigraphic data to determine the hard rock percentage of the overlying strata.

**AU2 mine:** The AU2 mine operates with a seam thickness from 2.9 to 4.2 m, and the seam thickness is approximately 3.6 m at the monitoring site. The stratigraphic sequence can be seen in Fig. 2. A sandstone and siltstone unit overlies the coal seam. A thick clay unit overlies a clay/sand sequence followed by basalt with a varying thickness. The overburden depth above the instrumentation site is around 125 m. The panel width is 280 m and the chain pillars are on  $35 \times 130$  m centers with 5-m entry widths. The hard rock ratio is calculated as 48% for this mine.

**AU3 mine:** The seam thickness for the AU3 mine varies from 3.4 to 4.0 m, and a typical stratigraphic column near the instrumentation site is presented in Fig. 2. The seam is overlain mostly by sandstone with a couple of bands of siltstone and claystone. The hard rock percentage is calculated as 57%. The depth of cover is approximately 130 m, and the panel void width is 205 m. The chain pillars are on  $30 \times 125$  m centers with 5.2-m-wide roadways. There is a 1-m-thick clayey siltstone underlying the coal seam which deteriorates when exposed to water and traffic, so 50 cm of coal is left for maintaining good roadway conditions. Below the clayey siltstone, the lithology continues with strong layers of sandstone, shale, mudstone, and siltstone.

**AU4 mine:** At the AU4 mine, 4.8 m of coal is extracted. The overlying strata consist of layers of generally competent and strong layers of shale, sandstone, conglomerate, volcanic tuff and coal seams (Fig. 2). The depth of cover varies from 150 to 200 m where it is approximately 180 m at the instrumentation site. The 135-m-wide longwall panels are designed with  $31 \times 102$  m center chain pillars with 5-m-wide roadways. The hard rock ratio is around 33%. The floor of the seam mostly consists of sandstone with occasional thin shale units in some areas.

**AU5 mine:** The seam extracted at the AU5 mine is relatively flat and is 2.5 m in thickness. Overlying the seam, there is a 300-m-thick sequence of major sandstone and shale units. That sequence is overlain by a massive sandstone of 160 to 180 m in thickness. Fig. 2 has the visual representation of the stratigraphic column; however, it is generated from the description of the geology in a report without a core log. The overburden is approximately 475 m above the instrumentation site and can be considered 71% hard rock. The 205-m-wide panels are supported by  $42 \times 102$  m center chain pillars, and the roadway width is approximately 4.8 m. The immediate floor is around 1 m of carbonaceous siltstone underlain by a strong sandstone.

**AU6 mine:** The coal seam at the AU6 mine is 6.5-m-thick, but the development thickness is 3.2 m. Immediately overlying the seam is a competent volcanic tuff layer of 1.49 m thickness. Sequence of shale and sandstone layers follow with some minor coal seams. There is a very strong sandstone/conglomerate unit lying 15–18 m above the roof (Fig. 2). The depth of cover varies from 220 to 280 m with 240 m adjacent to the instrumentation site with around 23% of hard rock. The 150-m-wide panels are separated by chain pillars on 35-m-centers with 5-m-wide roadways. The immediate floor is 4-m-thick shale underlain by interbedded sandstones and shales.

AU7 mine: The AU7 mine operates at a depth of cover of 405 m with a variable seam thickness from 1.8 to 3.7 m. The panel widths are 200 to 250-m-wide (rib to rib), and they are supported by 48-m-wide chain pillars, which have 5.2-m-wide nominal cut-throughs at 100-m centers. The overlying strata mostly consist of sandstone intermixed or interbedded with siltstone (Fig. 2) that produced about a 21% hard rock ratio.

AU8a-b mine: Two sets of measurements were taken from the AU8 mine. The depth of cover changes from 500 to 535 m. The seam thickness varies from 5 to 6.6 m. The overlying strata mostly consist of thick sandstone layers and siltstone giving a 72% and 95% hard rock ratio, respectively (Fig. 2). The immediate floor and roof have conglomerate units. The measurements are taken next to two different panels that are 227 and 237 m wide, respectively. Chain pillars are 45-m-wide with 5-m-wide entries for the 227-m-wide panel and for the 237-m-wide panel, the chain pillars are 60-m-wide with 6-m-wide entries.

AU9 mine: The depth of cover for the AU9 mine typically ranges from 300 to 350 m. A sandy soil cover of 1 to 5 m depth overlies a low-to-very-low strength, highly weathered sandstone on the surface. Highly competent and massive sandstone units exist between depths of 50 to 200 m (Fig. 2). The panel extracted adjacent to the instrumentation site is 250-m-wide with an extraction height of 6.7 m, and the chain pillars are 43-m-wide, rib to rib with 5-m-wide roadways. The hard rock ratio is calculated as 61%.

US1a-b mine: Two sets of measurements were collected from the US1 mine where the overburden depths were 595 and 625 m, respectively. The panels are supported by 6-m-wide yield pillars on both sides of 24-m-wide chain pillars. First measurements are taken next to a 195-m-wide panel, while the other set of measurements are collected next to a 183-m-wide panel. The hard rock ratio of the overlying strata was calculated as 54%. The strength and stiffness of the surrounding strata of the coalbed are uncommonly high for coal measure rocks. Except for the dark-gray shale, all the rock types have uniaxial compressive strength (UCS) values from 197 to 120 MPa. The absence of roof and floor fractures or joints together with the thick sandstone result in a hard-to-break main roof and greater pillar loads at this site [19].

## 4. Abutment angle analysis

### 4.1. Back-calculation of abutment angles

In-situ stress measurements constitute the stress profiles. A sample stress profile plotted using the measured values can be seen in Fig. 3. Fig. 3 represents the stress change profile of a two-entry system where the measurements were taken from the pillars and the adjacent solid coal. The area  $L_A$  represents the abutment load on the gateroad pillar, and the area  $L_B$  represents the abutment load on the adjacent solid coal. The areas  $L_A$  and  $L_B$  were numerically calculated by integrating the load under the curve.

Tulu and Heasley have explained the back-calculation for laminated overburden stress distribution approach in detail, and the same procedure is used for calculating the abutment loads in this study [8].

Finally, the value of the abutment angle is back calculated from the ratio of abutment load to total panel load according to the subcritical or supercritical panel formulas. Considering available subsidence information to determine the panel condition (subcritical or supercritical) will help give a more precise result. Where available, this information was taken into account in this study.

The back-calculated abutment angles are shown in Table 4. The results show that for deeper mines, the abutment angle was lower than the average 21° abutment angle used in ALPS and ARMPS2010.

#### 4.2. Regression analysis for abutment angle

Next the hypothesis that there was a correlation between the geology and the abutment angle was tested. Fig. 4 shows the calculated abutment angles with respect to panel width to overburden depth ratios, with the hard rock percentages as color coding. The blue points represent the cases that have hard rock ratios higher than 80%, and the yellow points represent the cases that have hard rock ratios between 50% and 80%. The red points represent the cases with less than 50% hard rock in the overlying strata. There was not any apparent significance of the percentage hard rock on the abutment angle. The only visible finding was some clustering of stronger overburden cases at lower abutment angles. More comprehensive geological analysis with additional geological information is needed for a better conclusion.

Fig. 5 shows the results for the abutment angles back calculated using the laminated model together with previously calculated cases [1,3,17]. For the mines deeper than 200 m, the abutment angle values are distributed from the maximum value of 23.4° to the minimum value of 4.7°, with the mean of 12.2°. For the mines with overburden depth less than 200 m, the scatter is much larger, but the average abutment angle of 21° is appropriate to assume.

As seen in Fig. 6, there is also an apparent trend of decreasing abutment angles with increasing ratios of overburden depth to panel width ( $\frac{H}{PW}$ ). A regression analysis to determine the abutment angle for deep cover cases ( $H > 200$  m) is conducted. The 200 m is selected as the limit depth, since the large data scatter occurs for shallower cases. The value is also reasonable to be considered as the boundary between deep and shallow mines [5].

For the regression analysis, the  $\frac{H}{PW}$  ratio was found to be the most significant parameter for determining the abutment angle, and the following equation is proposed:

$$\beta = a \times b \frac{H}{PW} \quad (1)$$

where  $\beta$  is the abutment angle.

Based on the field data analyzed in this paper, the proposed abutment angle determination is shown as the red line in Fig. 7. When the overburden depth is less than 200 m, a constant abutment angle of 21° is still applicable. With an overburden depth from 200 to 625 m, an abutment angle (b) that decreases with a continuous function of the  $\frac{H}{PW}$  ratio is proposed

(Table 5). This equation was derived by performing a least-square error fit to the measured abutment angles above 200 m overburden depth. Almost all the cases deeper than 200 m also have an  $\frac{H}{PW}$  ratio more than 1. The new equation should be considered applicable inside the range of the case studies ( $0.7 < \frac{H}{PW} < 3.5$ ).

#### 4.3. Logistic regression analysis for database classification

In order to confirm its applicability, the new abutment angle equation was tested on the case histories that were used for the development of the ARMPs2010 design criteria. The stability factors for 640 cases were calculated using both the ARMPs2010 and ARMPs-LAM programs. The database used for the analysis includes 640 cases, of which 520 were successful and 120 were failed case histories. The failed cases include: 14 collapses, 81 squeezes, 16 multipillar bursts, and 9 local bursts. The analyses aimed to compare the new abutment angle equation with the classification success of the ARMPs2010 design criteria. The failure classification rates of the ARMPs2010 design criteria were matched and compared.

First, shallow cases ( $H \leq 2000$  m) were tested considering the ARMPs2010 design criteria of ARMPs2010 SF of 1.5. The ARMPs2010 SF refers to the SF of pillars inside the active mining zone (AMZ) as a whole. The ARMPs2010 classification rates are given in Table 6. Of the 204 shallow cases, 46 of them are failed cases with 28 squeezes and 14 pillar collapses. Out of the 46 failed cases, ARMPs2010 design criteria successfully classified 42 of them (91%). The 4 failed cases that were classified falsely include only pillar squeezes. The 133 of the 158 (84%) successful cases were also classified correctly by the design criteria (Fig. 8).

SF values for the same case histories were also calculated by ARMPs-LAM using the new abutment angle equation. Since the new abutment angle equation was proposed for deep cover cases, both programs used the original  $21^\circ$  abutment angle. The limit SF value was determined as 1.84, so that the classification accuracy of failed cases is set to be 91% and is the same as the ARMPs2010 classification accuracy. This suggests that if one uses ARMPs-LAM for design purposes, 1.84 should be taken as the limit SF. The results are given in Table 7. The classification accuracy of the successful cases was slightly reduced from 84% down to 83%. Also, one pillar collapse and three pillar squeezes (Fig. 9) were classified falsely compared to ARMPs2010 that only misplaced pillar squeezes. It can be concluded that, for shallow cases, almost identical separation was achieved with the ARMPs-LAM program.

A second set of analyses was conducted using the 215 deep cover case histories that utilize barrier pillars. Out of those 215 cases, 182 of them were successes and the remaining 33 were failures. These cases were initially analyzed using  $21^\circ$  abutment angle and standard ARMPs2010 design criteria that use 1.5 for both ARMPs2010 SF and barrier pillar (BP) stability factor (SF) values. Corresponding classification accuracies are given in Table 8. The ARMPs2010 design criteria correctly classified 29 of 33 failures (88%) and 61 of 182 successful cases (34%). Out of the 4 falsely classified cases, one of them was a local pillar burst, and the other three were pillar squeezes (Fig. 10).

The same case histories (deep cover with BP) are reanalyzed using the ARMPs2010 program with the new abutment angle equation (Table 5) instead of the constant  $21^\circ$ . In order to provide a failure classification accuracy of 88%, the ARMPs2010 SF was kept as 1.5 and BP SF value is determined as 2.15. As seen in Table 9, classification of successful cases increased notably up to 43% (78 out of 104). Failure types of the falsely classified failed cases remained unchanged (1 local burst and 3 squeezes).

Both the active mining zone (AMZ) and BP SF values were calculated for the same 215 cases using ARMPs-LAM with the abutment angle calculated with the new suggested equation. A minimum of 88% accurate failure classification is targeted for the limit SF values to be considered. That classification accuracy is achieved with an AMZ SF of 1.45 and BP SF of 2.2. An 88% failure classification accuracy is achieved with a success classification accuracy of 46% (Table 10).

As seen in Fig. 11, ARMPs-LAM only misclassified pillar squeezes, where ARMPs2010 design criteria misclassified a local burst failure in addition to pillar squeezes. Although pillar squeezes cause hazardous situations, the fact that they develop slowly (where collapses and bursts occur with little or no warning) makes it easier to react to the situation and abandon the area [5].

The classification accuracies of both ARMPs2010 and ARMPs-LAM for different cases are presented in Table 11. The failure classification accuracy of ARMPs-LAM was targeted to be at least as good as that of ARMPs2010 for the same cases. More than 80% of the cases that utilize barrier pillars are deep cover cases, so we can say that ARMPs-LAM, used together with the new abutment angle equation, gives considerably better results for deep cover cases. Since the shallow cover cases are not included in the new abutment angle equation, those can be considered for the comparison of ARMPs2010 and ARMPs-LAM.

For deep cover cases, an ARMPs-LAM SF of 1.45 and BP SF of 2.2 were found to be applicable when the new abutment angle equation is used together with the laminated model. However, if ARMPs-LAM is used for shallow cover cases, the limit ARMPs-LAM SF should be taken as 1.84.

## 5. Conclusions

The ARMPs2010 design software for retreat mining pillar design uses the empirically derived abutment angle of  $21^\circ$  that was derived from field studies conducted in the mid-1980s and through the 1990s [12,20]. Modern mine designs use significantly different panel depths and widths compared to these cases. In this paper, traditional calculations for abutment loading are reexamined using a current database of more recent in-situ stress measurements from 12 full case studies with an additional 18 supplementary case studies.

The re-analysis of the abutment angles presented in this paper showed that for higher overburden depths, the re-analyzed abutment angle appeared to be much less than the traditionally used  $21^\circ$  abutment angle. Based on the field data analyzed in this paper, researchers propose a new abutment angle calculation that considers depth to panel width ratio (see Table 5). When the overburden depth is less than 200 m, the  $21^\circ$  abutment angle

proposed by Mark still holds its applicability [12]. It is known from the ARMPs2010 analysis that the 21° abutment angle works fine for the shallow cover cases [5]. However, from depths of 200 to 625 m, the abutment angle calculated with the equation in Table 5 should be considered.

Using the proposed new abutment angle equation, cases used to develop ARMPs2010 were re-analyzed with the ARMPs-LAM software. It was observed that the ARMPs2010 design criteria was slightly better at classifying the cases when the shallow cover database is considered. However, when the deep cover cases are considered separately, the classification accuracy of ARMPs2010 is improved with the newly proposed abutment angle equation. If the deep cover cases with a barrier pillar are considered separately, 88% of the failed cases and 46% of the successful cases were correctly classified by ARMPs-LAM compared to using a constant 21° abutment angle (88% and 34% respectively). It can be concluded that, for deep cover cases, a better separation can be achieved by the new abutment angle equation. Also, the ARMPs-LAM program gave better separation for deep cover cases and was almost equally successful when shallow cover cases were considered. The fact that ARMPs-LAM provides a real mechanical explanation for the load transfer is an important factor to be considered in mine layout design. ARMPs-LAM software can be considered as a design tool, especially for deep cover ( $H > 200$  m) cases that use barrier pillars with the implementation of the newly proposed abutment angle equation. For deep cover cases, an ARMPs-LAM SF of 1.45 and BP SF of 2.2 were found to be applicable when the new abutment angle equation is used together with the laminated model. However, if ARMPs-LAM is used for shallow cover cases, the limit ARMPs-LAM SF should be taken as 1.84.

Finally, in this study, there was no apparent relationship between the hard rock ratio and the abutment angle, which might be due to insufficient information about the overlying strata. Since there is no doubt that the overburden geology plays an important role in load distribution around the panels, a more comprehensive investigation with detailed geological information is planned to be conducted in the future.

## Acknowledgements/Disclaimers

This study was sponsored by the Alpha Foundation for the Improvement of Mine Safety and Health, Inc. (ALPHA FOUNDATION). The views, opinions and recommendations expressed herein are solely those of the authors and do not imply any endorsement by the ALPHA FOUNDATION, its Directors and staff. The findings and conclusions in this report are those of the author(s) and do not necessarily represent the official position of the National Institute for Occupational Safety and Health, Centers for Disease Control and Prevention. Mention of any company or product does not constitute endorsement by NIOSH.

## References

- [1]. Mark C Pillar design methods for longwall mining. Bureau of Mines: US Department of the Interior; 1990.
- [2]. Mark C, Chase FE. Analysis of retreat mining pillar stability. In: Proceedings of the NIOSH technology transfer seminar NIOSH; 1997 p. 17–34.
- [3]. Colwell M, Frith R, Mark C. Analysis of longwall tailgate serviceability (ALTS): a chain pillar design methodology for Australian conditions. In: Proceedings of the 2nd international workshop on coal pillar mechanics and design NIOSH; 1999 p. 33–48.
- [4]. Mark C. West Virginia University. Deep cover pillar recovery in the US; Proceedings of the 28th international conference on ground control in mining; Morgantown. 2009. 1–9.

[5]. Mark C. West Virginia University. Pillar design for deep cover retreat mining; Proceedings of the 3rd international workshop on coal pillar mechanics and design; Morgantown. 2010. 106–22.

[6]. Heasley KA. Numerical modeling of coal mines with a laminated displacement- discontinuity code. In: Doctoral dissertation Golden: Colorado School of Mines; 1999 p. 80.

[7]. Heasley KA, Sears MM, Tulu IB, Calderon-Arteaga CH, Jimison LW. Calibrating the LaModel program for deep cover pillar retreat coal mining. In: Proceedings of the 3rd international workshop on coal pillar mechanics and design Morgantown: West Virginia University; 2010 p. 47–57.

[8]. Tulu IB, Heasley KA. Investigating abutment load. In: Proceedings of the 31st international conference on ground control in mining Morgantown: West Virginia University; 2012 p. 1–10.

[9]. Tulu IB, Heasley KA, Mark C. A comparison of the overburden loading in ARMPS and LaModel. In: Proceedings of the 29th international conference on ground control in mining Morgantown: West Virginia University; 2010 p. 28–37.

[10]. Zhang P, Heasley KA, Agioutantis ZG. A comparison between ARMPS and the new ARMPS-LAM programs. In: Proceedings of the 33rd international conference on ground control in mining Morgantown: West Virginia University; 2014 p. 170–4.

[11]. Mark C Analysis of longwall pillar stability. In: Doctoral dissertation State College: The Pennsylvania State University; 1989 p. 10–20.

[12]. Mark C. US Department of the Interior, Bureau of Mines. Analysis of longwall pillar stability (ALPS): an update; Proceedings of the workshop on coal pillar mechanics and design; Pittsburgh (PA). 1992. 238–49.

[13]. Vandergrift T, Conover D. Assessment of gate road loading under deep Western US conditions. In: Proceedings of the 3rd international workshop on coal pillar mechanics and design Morgantown: West Virginia University; 2010 p. 38–46.

[14]. Lawson HE, Tesarik D, Larson MK, Abraham H. Effects of overburden characteristics on dynamic failure in underground coal mining. *Int. J. Min. Sci. Technol* 2017;27(1):121–9.

[15]. Reed G, McTyre K, Frith R. An assessment of coal pillar system stability criteria based on a mechanistic evaluation of the interaction between coal pillars and the overburden. *Int. J. Min. Sci. Technol* 2017;27(1):9–15.

[16]. Van Dyke MA, Su wH, Wickline J. Evaluation of seismic potential in a longwall mine with massive sandstone roof under deep overburden. *Int. J. Min. Sci. Technol* 2018;28(1):115–9. [PubMed: 30027000]

[17]. Hill D Personal communications. 2016.

[18]. Agioutantis Z, Karmis M. Quick reference guide and working examples. In: Surface Deformation Prediction System for Windows. p. 330.

[19]. Campoli AA, Barton TM, Van Dyke FC, Gauna M. Gob and gate road reaction to longwall mining in bump-prone strata. US Department of the InteriorBureau of Mines Report of Investigations, 1993.

[20]. Peng SS, Chiang HS. Longwall Mining. New York: Wiley & Sons; 1984.

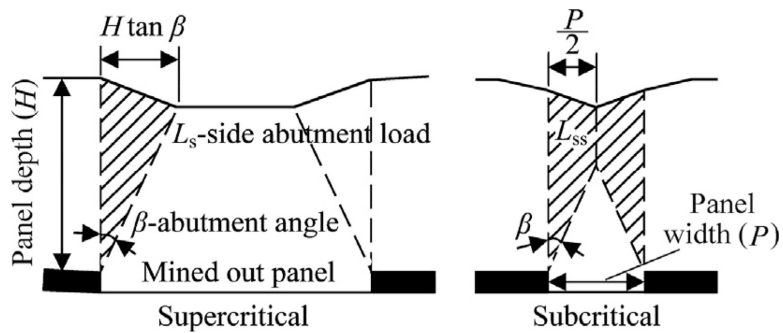


**Fig. 1.**  
Abutment angle concept (after [12]).

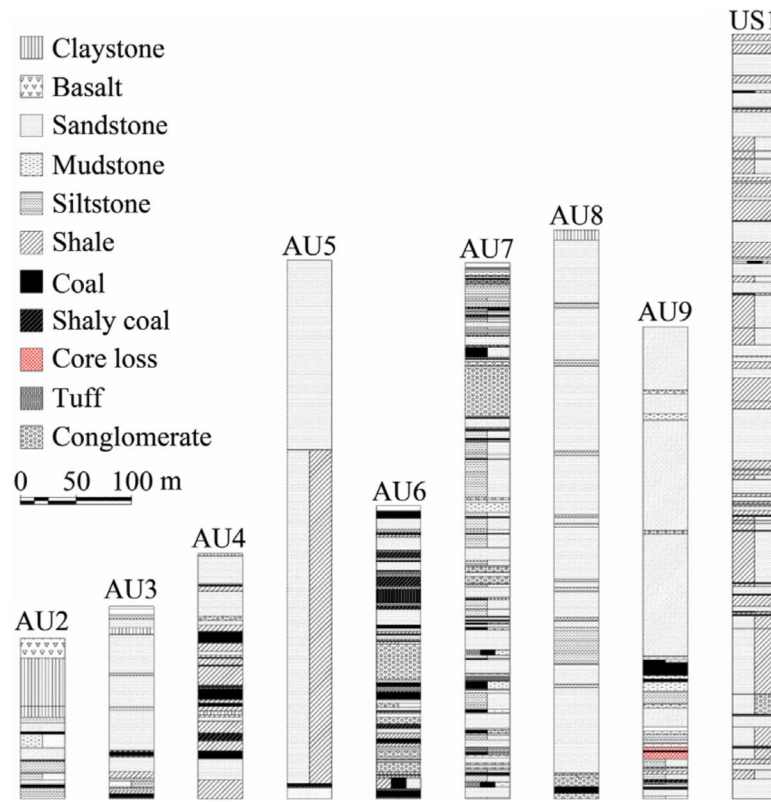


**Fig. 2.**  
Generalized stratigraphic column representation of the mines.

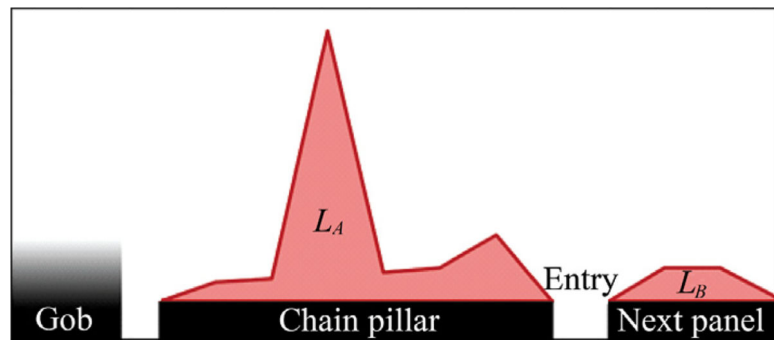


**Fig. 3.**  
Sample stress profile from a two-entry mine.

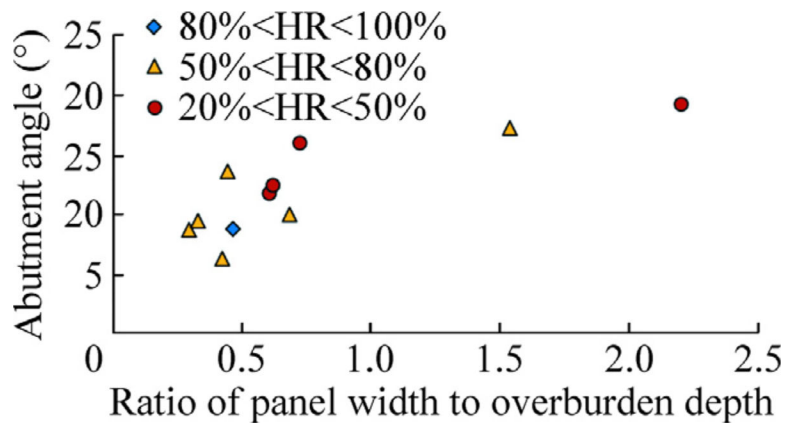


**Fig. 4.**

Abutment angles calculated using the laminated model with respect to panel width to overburden depth ratios together with hard rock percentages.

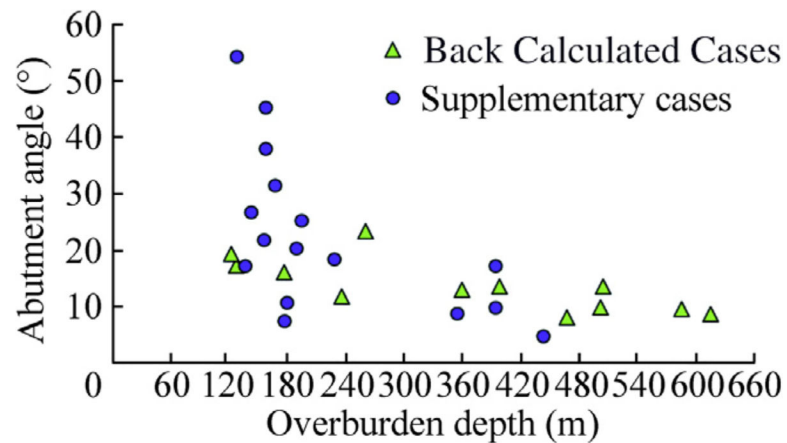


**Fig. 5.**

Determined abutment angles with respect to overburden depths.

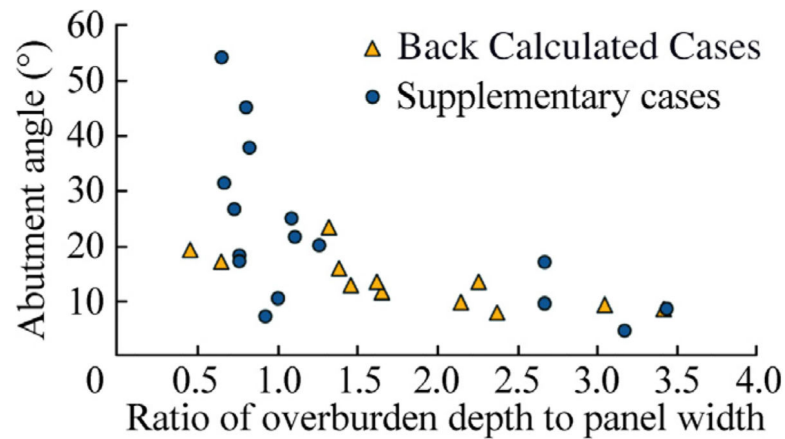


**Fig. 6.**

Determined abutment angles with respect to overburden depth to panel width ratios.

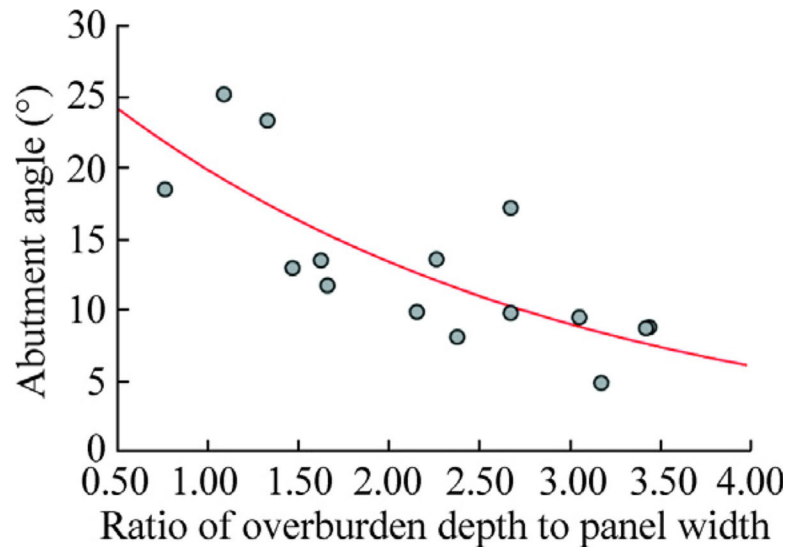


**Fig. 7.**

New abutment angle model for deep cover cases ( $\beta = 29.42 \times 0.68 \frac{H}{PW}$ ).

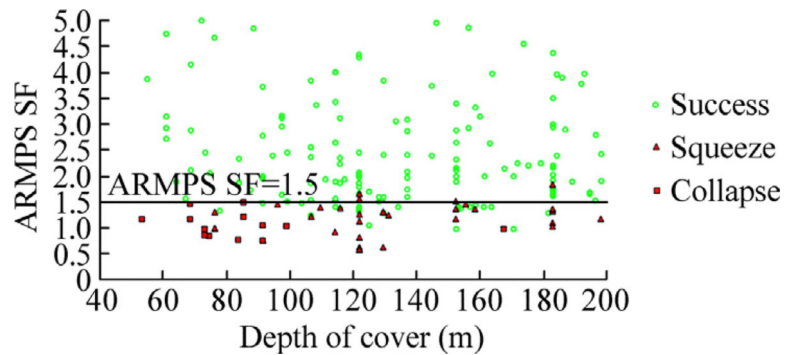


**Fig. 8.**  
ARMPS2010 SF results of the ARMPS2010 shallow cover database using the 21° abutment angle.

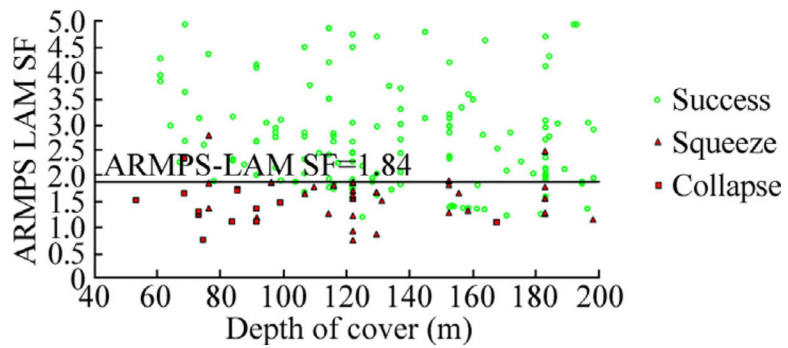


**Fig. 9.**  
ARMPS-LAM SF results of the ARMPS2010 shallow cover database using the 21" abutment angle.

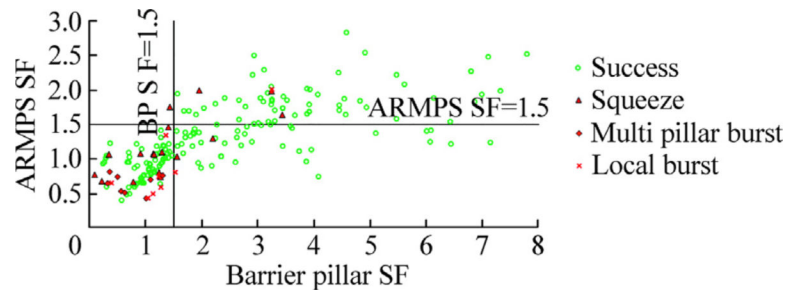


**Fig. 10.**

ARMPS2010 SF values for deep cover cases that utilize BP using  $21^\circ$  abutment angle.

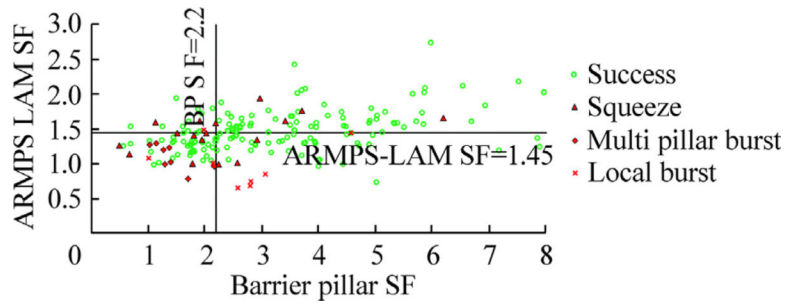


**Fig. 11.**  
ARMPS-LAM classification capability for deep cover cases using the new abutment angle equation.

**Table 1**

Summary of the stress measurement sites used [1].

Case	Panel depth (m)	Panel width (m)	Seam	Abutment angle (°)
Mine A:2	159	143	Pittsburgh	21.8
Mine B:2	198	183	Pittsburgh	25.2
Mine B:3	183	183	Pittsburgh	10.7
Mine B:4	139	183	Pittsburgh	17.3
Mine D:1	232	305	Lower Kittanning	18.5
Mine E:3	192	153	Harlan	20.3
		Average		19.0

**Table 2**

Summary statistics of the present stress measurement database.

Parameter	Cover depth (m)	Panel width (m)	Ratio of width to depth
Average	289	191	0.83
Standard deviation	158	44	0.43
Minimum	125	105	0.29
Maximum	625	305	2.20

**Table 3**

Summary of mine geometries for the new cases.

Case	Depth(m)	Panel width (m)	Seam thickness (m)	Entry width (m)	HR (%)
AU-1	265	205	2.5	5.1	N/A
AU-2	125	280	3.6	5	48
AU-3	130	205	3.1	5.2	57
AU-4	180	135	3.2	5	33
AU-5	475	205	2.5	4.8	71
AU-6	240	150	6.5	4.9	23
AU-7	405	250	2.5	5.2	21
AU-8a	513	227	5.5	5	72
AU-8b	510	237	5.5	6.1	95
AU-9	365	250	6.7	5	61
US-1a	594	195	1.7	6.1	54
US-1b	625	183	1.7	6.1	54

**Table 4**

Back-calculated abutment angles.

Case	Abutment angle (°)	Overburden depth (m)	Panel width (m)
AU-1	23.39	265	200
AU-2	19.30	125	275
AU-3	17.24	130	200
AU-4	16.03	180	130
AU-5	6.33	475	200
AU-6	11.79	240	145
AU-7	12.48	405	250
AU-8a	13.62	513	227
AU-8b	8.85	510	237
AU-9	10.00	365	250
US-1a	9.51	594	195
US-1b	8.74	625	183

**Table 5**

Proposed abutment angle equation for  $\frac{H}{PW}$  ratios from 0.7 to 3.5.

Overburden depth (m)	Abutment angle (°)
$H = 200 \text{ m}$	$21^\circ$
$200 \text{ m} \leq H \leq 625 \text{ m}$	$\beta = 29.42 \times 0.68 \frac{H}{PW}$

**Table 6**

Classification accuracies of ARMPS2010 SF of 1.5 for shallow mines using 21° abutment angle.

Type	Success observed	Failure observed	Total
Success classified	133	4	137
Failure classified	25	42	67
Total	158	46	204
Accuracy (%)	84	91	86

**Table 7**

Classification accuracies of ARMPS-LAM SF of 1.84 for shallow mines using 21° abutment angle.

Type	Success observed	Failure observed	Total
Success classified	131	4	135
Failure classified	27	42	69
Total	158	46	204
Accuracy (%)	83	91	85

**Table 8**

Classification accuracies for deep cover cases of ARMPS2010 SF and the BP SF of 1.5 using the 21° abutment angle.

Type	Success observed	Failure observed	Total
Success classified	61	4	65
Failure classified	121	29	150
Total	182	33	215
Accuracy (%)	34	88	42

**Table 9**

Classification accuracies for deep cover cases using the new abutment angle equation using the ARMP2010 program with ARMP2010 SF of 1.5 and BP SF of 2.15.

Type	Success observed	Failure observed	Total
Success classified	78	4	82
Failure classified	104	29	133
Total	182	33	215
Accuracy (%)	43	88	50

**Table 10**

Classification accuracies for deep cover cases of ARMPS-LAM SF of 1.45 and BP SF of 2.2 using the new abutment angle equation.

Type	Success observed	Failure observed	Total
Success classified	84	4	88
Failure classified	98	29	127
Total	182	33	215
Accuracy (%)	46	88	53

ARMPS2010 and ARMPS-LAM classification accuracies for different sets of cases.

Case	Number	Failure classification accuracy (%)	ARMPS2010 success classification accuracy (%)	ARMPS-LAM success classification accuracy (%)
All	640	82	59	55
Shallow cover	204	91	84	82
Deep cover	436	94	16	23
Deep cover with side gob	249	92	30	42
Deep cover with barrier pillar	215	87	33	46